

1 Heuristic Algorithms for Design of Integrated Monitoring of

2 Geologic Carbon Storage Sites

3 Alexander C. Hanna^a, Jonathan Whiting^a, Brian Huang^a, Delphine Appriou^a, Xianjin Yang^b,
4 Julia de Toledo Camargo^a, Seunghwan Baek^a, Diana Bacon^a, Catherine Yonkofski^a

^a*Pacific Northwest National Laboratory, Richland, WA 99354*
^b*Lawrence Livermore National Laboratory, Livermore, CA 94550*

7 Abstract

8 The Designs for Risk Evaluation and Management (DREAM) tool was developed as part
9 of the effort to quantify the risk of lack of containment for geologic storage of carbon dioxide
10 (CO_2) under the U.S. Department of Energy's National Risk Assessment Partnership (NRAP).
11 DREAM is an optimization tool created to identify optimal monitoring schemes that minimize
12 the time to first detection of CO_2 leakage from a subsurface storage formation. DREAM acts as
13 a post-processor on user-provided output from subsurface leakage simulations. While DREAM
14 was developed for CO_2 leakage scenarios, it is applicable to any subsurface leakage simulation
15 of the same output format. The DREAM tool is comprised of three main components: (1) a Java
16 wizard used to configure and execute the simulations, (2) a visualization tool to view the domain
17 space and optimization results, and (3) a plotting tool used to analyze the results. A secondary
18 Java application is provided to aid users in converting common American Standard Code for
19 Information Interchange (ASCII) output data to the standard DREAM hierarchical data format
20 (HDF5). DREAM employs a simulated annealing approach that searches the solution space by
21 iteratively mutating potential monitoring schemes built of various configurations of monitoring
22 locations and leak detection parameters. This approach has proven to be orders of magnitude
23 faster than an exhaustive search of the entire solution space. The user's manual illustrates the
24 program graphical user interface (GUI), describes the tool inputs, and includes an example ap-
25 plication.

The latest version of the software, DREAMv3.0, introduces the ability to optimize surface geophysical surveys taken over various areas of the field site at irregular intervals. This optimization can be run using surface geophysics only, wellbore instruments only, or using a combination of surface geophysical surveys and wellbore instruments. These two approaches generally have broadly overlapping sensitivities, as a surface geophysical survey detects over a wide area of the field but only detects signals that are detectable along the surface at the time the survey was conducted, whereas a wellbore sensor can generally detect signals in the subsurface continuously the entire time it is in place, but only at one point in space. Therefore a pairing of wellbore sensors limited in their spatial coverage with geophysical surveys limited in their temporal coverage can produce a much improved monitoring plan. This software assumes that a set of hypothetical simulated CO₂ leaks are available, and that those leaks are representative of the underlying risk profile for a site. This allows the software to remain lightweight and functional on a typical laptop, and reduces the barrier to entry for users who lack the expertise of budget for high performance computing. This also improves compatibility across various application domains, allowing the tool to remain independent from any software dependencies related to for-

41 ward modelling or model calibration. Leak scenarios can be provided in the HDF5 file format,
42 as NRAP-Open-IAM output files, or as STOMP, NUFT, Tecplot or Tough2 simulation files.

43

44 **Keywords:** carbon sequestration, subsurface monitoring design, gravity surveys, optimization,
45 genetic algorithms

46 **1. Introduction**

47 Geological carbon capture and storage is one proposed means of mitigating human-induced
48 climate change, by diverting and concentrating anthropogenic point sources of carbon dioxide
49 into a supercritical fluid and then injecting it into a permeable underground rock formation for
50 long-term storage. One application of this technique is in enhanced oil recovery, where the
51 physicochemical properties of supercritical CO₂ are used as a solvent to strip oil from mineral
52 grain surfaces and mobilize it towards an oil production well. Another financial incentive for
53 industry to pursue this technology is 45Q tax credits, which allow private industry to receive
54 tax credits for capturing and storing carbon dioxide rather than releasing it into the atmosphere.
55 This tax credit is currently priced at \$10-20 per metric ton with some proposals to gradually
56 increase the price to \$35-50 per metric ton, and current CO₂ emissions are approximately 5
57 billion metric tons per year in the US. Therefore if monitoring costs and operational risks are
58 sufficiently minimized, geologic carbon storage can potentially become an industry on the order
59 of \$100 billion/year in the near future.

60 One of the main challenges of this endeavor is verifying that the stored carbon dioxide re-
61 mains stable and immobilized, as drilling enough monitoring wells near enough to the storage
62 reservoir to detect every possible combination of CO₂ leaks can be prohibitively expensive. The
63 DREAM (Designs for Risk Evaluation and Management) software package was therefore devel-
64 oped in order to design optimal arrays of monitoring wells. DREAM accepts an ensemble of
65 potential leak scenarios as input, and then develops a Pareto-optimal set of monitoring plans rep-
66 resenting the range of possible tradeoffs between cost and risk. DREAM is designed to maintain
67 a low technical barrier to entry, and can be run on a typical laptop or workstation rather than a
68 supercomputer.

69 The latest version of DREAM also incorporates a mix of direct monitoring through wellbores
70 as well as remote sensing through gravity surveys conducted along the surface. While incorpo-
71 rating gravity surveys can improve the cost and performance of the overall monitoring plan, it
72 can also make the optimization problem more challenging. Heuristic algorithms were therefore
73 developed to efficiently solve these mixed continuous-combinatorial optimization problems.

74 **2. Background**

75 The algorithmic design of optimized sensor networks for environmental monitoring is a well-
76 studied area of research [8, 10, 21], with many studies [17, 18, 19] focusing on simulated anneal-
77 ing [See Section 3.2.3] while others [5, 6, 7, 12, 14, 20, 24] use genetic algorithms [See Section

*Corresponding author. Tel.: +1 (509) 375-5945

Email address: alexander.hanna@pnnl.gov (Alexander C. Hanna)

78 3.2.4]. The goal of the DREAM software [2, 25, 26, 27] has been to integrate these methods into
79 a single, user-friendly interface that uses a modular approach allowing it to be integrated into any
80 arbitrary forward modeling and history matching workflow.

81 **3. Methods**

82 *3.1. Software Application*

83 This software is written primarily in Java, and has a graphical user interface with a series
84 of windows allowing the user to configure the knowns, unknowns and constraints of their moni-
85 toring design problem. The software accepts a set of hypothetical simulated CO₂ leakage files
86 as inputs, and treats those leakage files as representative of the underlying risk profile for a site.
87 Leak scenarios are composed of physical parameters such as pore pressure, CO₂ concentration,
88 or salinity as a function of x,y,z and time, and can be provided in the HDF5 file format, as
89 NRAP-Open-IAM output files, or as STOMP, NUFT, Tecplot or Tough2 simulation files.

90 Once the leak ensemble is loaded into DREAM, the user defines leakage thresholds indicating
91 the value at which each subsurface parameter constitutes an impact or degradation to the aquifer.
92 For some values such as pore pressure, there may not be a value that harms the aquifer, whereas
93 other values such as salinity might be based on an MCL (Maximum Contaminant Level) defined
94 by a state or federal agency. The user then defines detection thresholds for each parameter, which
95 may be based off of the sensitivity of the instrument or the background noise levels particular
96 to the site. A distinction is made between leakage thresholds and detection thresholds, as the
97 amount of a given contaminant needed to impact an aquifer can be different from the amount
98 needed for its presence to become detectable.

99 The user can then define a set of weighting coefficients which guide the software in prioritiz-
100 ing sensor coverage for each leak. By default these weights are set equal, however they can be
101 re-defined based on the volume of aquifer degraded according to the leakage thresholds, or by a
102 user-supplied estimate of the relative probability of each leak occurring or the relative magnitude
103 or impact of each leak. These values can be defined manually within the GUI, or by reference
104 to an external csv file. There is also a collection of Python scripts available which parse the
105 csv files along with the input HDF5 files to generate visualizations of the optimization results as
106 static images files.

107 *3.2. Optimization Algorithms*

108 For each optimization algorithm, we programmatically develop a series of monitoring plans
109 each including a variety of wellbores, sensors and gravity surveys as well as their locations and
110 timings, and we then assess how each plan performs in terms of our monitoring objectives. The
111 five objectives available to consider are

- 112 1. Minimizing the purchasing, labor, installation and operational costs of the monitoring plan.
- 113 2. Maximizing the number of leak scenarios that would be detectable by the monitoring plan.
- 114 3. Maximizing the total mass of CO₂ of the leak scenarios that would be detectable by the
115 monitoring plan.
- 116 4. Minimizing the time to detect our leak scenarios.

117 5. Minimizing the volume of aquifer degraded at the time of detection.

118 These objectives broadly overlap in some cases, however they can also conflict with one
119 another to various degrees. For example, objective 1 conflicts strongly with objectives 2-5, as
120 improving any of those objectives almost always requires more sensors and boreholes drilled.
121 Objectives 2 and 3 also tend to conflict with objective 4, as detecting leak scenarios as early
122 as possible requires locating sensors very near their points of origin which tends to preclude
123 also detecting a large number of different potential leaks. Objectives 4 and 5 tend to correlate
124 strongly with one another, however they can also conflict at times. For example a small, high-
125 concentration but slow-moving leak may exceed the lower detection limits of our sensors and
126 become detectable very quickly, but may take a long time for the plume to expand and contami-
127 nate a large volume of the aquifer. By contrast, a fast-moving but low concentration plume may
128 contaminate a large area of the aquifer before finally reaching a high enough concentration to be
129 detectable by our sensors.

130 A tradeoff surface therefore exists, representing the range of compromises that can be made
131 between these five objectives. Some possible monitoring plans would provide a lot of broad
132 coverage and would eventually detect most or all of the potential leaks, while others may provide
133 more targeted coverage to preferentially detect the largest, most impactful (in terms of volume
134 of aquifer degraded) and the most likely leaks as quickly as possible, while others make some
135 compromises on coverage to minimize operating costs. Understanding the structure of this five-
136 dimensional Pareto-optimal surface is critical to making good site monitoring decisions.

137 *3.2.1. Grid Search*

138 An exhaustive grid search requires that we employ some combinatorics to evaluate every pos-
139 sible combination of sensor type and sensor location. We consider installing ${}_nC_r$ combina-
140 tions of sensors, where n is the number of sensor types we install and r is the number of sensors we
141 propose to install. This can be represented by the equation

$${}_nC_r = \frac{n!}{r!(n-r)!}, \quad (1)$$

142 which can itself quickly become computationally intractable if a large array of sensors are
143 needed. For example, if we consider employing three distinct sensor types (pressure, satura-
144 tion, gravity) and intend to install 5 sensors in total, we get 21 possible combinations

$$\text{Sensor Types} = \left\{ \begin{array}{ccccc} p & p & p & p & p \\ p & p & p & p & s \\ p & p & p & p & g \\ p & p & p & s & s \\ \dots & \dots & \dots & \dots & \dots \\ s & s & g & g & g \\ s & g & g & g & g \\ g & g & g & g & g \end{array} \right\}, \quad (2)$$

145

146

147 however if we consider installing 15 sensors, that leads to 136 possible sensor combinations.

148 We then consider the list of possible sensor locations, as discretized by the xyz grid used in our
149 ensemble of leak scenario files. Many of these grid nodes can be neglected, as they never see

150 a signal that exceeds the threshold and would never detect any of the leaks from the ensemble.
151 However, there may still be thousands to millions of feasible sensor location combinations.

$$\text{Node Locations} = \left\{ \begin{array}{ccccc} 0 & 0 & 0 & 0 & 0 \\ 0 & 0 & 0 & 0 & 1 \\ 0 & 0 & 0 & 0 & 2 \\ \dots & \dots & \dots & \dots & \dots \\ 20 & 20 & 21 & 21 & 21 \\ 20 & 21 & 21 & 21 & 21 \\ 21 & 21 & 21 & 21 & 21 \end{array} \right\}, \quad (3)$$

152
153
154 performing spatial downsampling on the aquifer simulation files can manage this to some degree,
155 but not without sacrificing some spatial resolution. We then compute the Cartesian product of
156 the list of possible sensor locations with the list of possible sensor location combinations. This
157 can readily lead to millions to trillions of possible monitoring plans, making it an impractical
158 approach for most full-reservoir models.

159 3.2.2. Monte Carlo

160 The Monte Carlo algorithm is a much simpler approach, randomly selecting the number and
161 locations of sensors at each iteration. While this is less thorough than the full grid search, it
162 tends to search the decision space fairly uniformly with a reasonable amount of computational
163 effort. In many cases this may quickly find the same ideal solution that would have eventually
164 been found by grid search.

165 3.2.3. Simulated Annealing

166 The Simulated Annealing algorithm [11, 16] begins by generating a single random moni-
167 toring plan, considering how well this plan would perform in terms of cost and leak detection,
168 then making a series of small, iterative modifications to this plan. At each iteration, it considers
169 whether the most recent change improved or degraded the monitoring plan performance, and
170 accepts the change if it was deemed an improvement. If the change degrades performance, a
171 random number generator is used to probabilistically accept or reject the change, with the accep-
172 tance probability depending on how much the performance was degraded. This encourages the
173 algorithm to occasionally "climb out" of a local minima and explore new areas of the decision
174 space. This algorithm can find "good" solutions very quickly, but often fails to find the best pos-
175 sible solution. It should generally be repeated multiple times to ensure that the decision space
176 has been adequately explored.

177 3.2.4. Non-dominated Sorting Genetic Algorithm II

178 The DREAMv3 NSGA-II option is based on the Non-dominated Sorting Genetic Algorithm
179 [4], which uses Pareto ranking [Figure 1] to iteratively develop a set of optimal monitoring plans.
180 Pareto ranking assigns each monitoring plan a rank based on how well it manages tradeoffs
181 between the various objectives, with rank 1 monitoring plans rated the best. In this example,
182 monitoring plans are being evaluated based on minimizing two objectives f_1 and f_2 . Monitoring
183 plans 1 and 2 [Figure 1a] are superior to monitoring plan 3 in terms of both objectives f_1 and
184 f_2 , and therefore they are both a lower (better) rank than plan 3. However, plan 1 and 2 are

185 ambiguous, as plan 1 is better in terms of objective f_1 while plan 2 is better in terms of objective
 186 f_2 . These two must therefore be assigned the same rank.

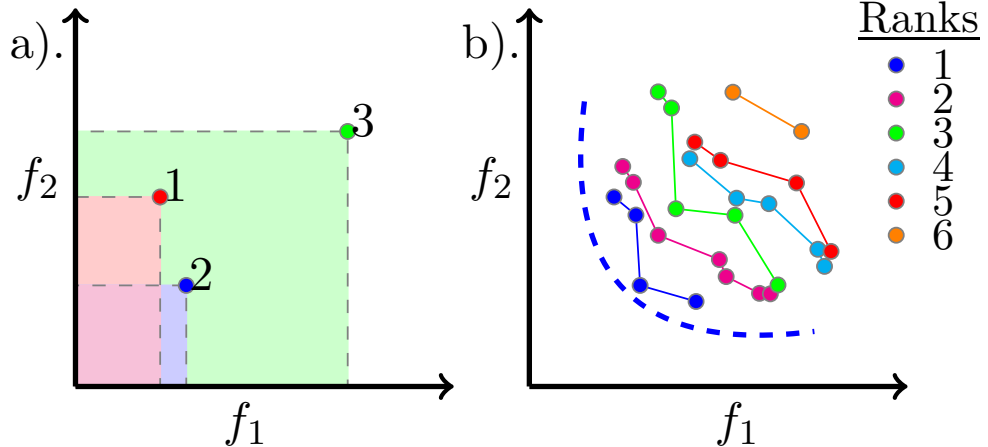


Figure 1: Illustration of Pareto optimality. Blue dashed line represents the 'true' Pareto front. Rank 1 solutions (blue dots) represent the best currently-available approximation of the Pareto front.

187 The NSGA-II algorithm uses a Monte Carlo approach to generate an initial population of
 188 monitoring plans, then semi-randomly selects pairs of monitoring plans from that ensemble.
 189 Monitoring plans with lower Pareto ranks are preferentially selected, and a de-clustering method
 190 is used to preferentially select monitoring plans that are more unique in terms of their objective
 191 values. Sensors from these pairs of monitoring plans are then randomly selected and used to
 192 construct new monitoring plans that often combine the best features of the "parent" pair. Over
 193 enough iterations, this generates a set of monitoring plans that evenly explore the Pareto front.

194 3.2.5. Heuristic Sampling

195 The DREAM heuristic algorithm divides the monitoring design problem into a sequence of
 196 sensor placement decisions. The first sensor is placed by evaluating the full set of available
 197 sensor placement locations in terms of the added drilling and installation costs, the number of
 198 hypothetical leaks that would be detectable at that location [Figure 2], and the average time to
 199 detection of those leaks. The algorithm then considers the tradeoff relationship between these
 200 objectives, and randomly selects one of the resulting Pareto-optimal locations as the first sensor
 201 placement. An example of the tradeoff relationship between two objectives is visualized in 2d in
 202 Figure 3, and between three objectives in 3d in Figure 4.

203 Once the first sensor location has been determined, the set of hypothetical leaks that would
 204 be detected by that sensor are neglected and the objectives are re-computed considering only the
 205 set of leaks that would not be detectable by the first sensor. This process is repeated many times
 206 with various numbers and types of sensors as indicated by the users specifications. Where surface
 207 geophysical survey methods are being considered, several (1-4, randomly selected) points along
 208 the surface are sequentially chosen in the manner described above, and a rectangular survey
 209 geometry is constructed so as to be just large and dense enough to include those points.

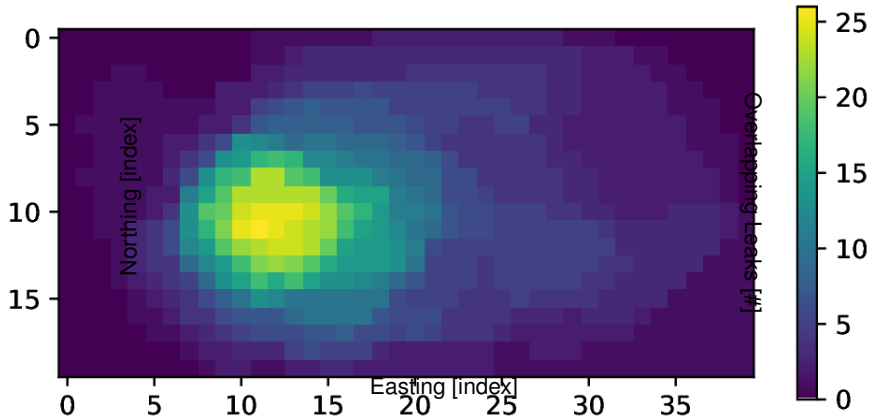


Figure 2: Color indicates the number of leaks that overlap at each point (x,y), considering only the leaks that as yet would be undetected by the current monitoring plan.

210 **4. Results**

211 *4.1. NRAP-Open-IAM FutureGen2 Aquifer ROM*

212 To create a set of leakage scenarios, a model of a hypothetical GCS site was created using the
 213 NRAP-Open-IAM [22], and integrated assessment model for quantifying the risk of unintended
 214 migration of CO₂ and brine out of a storage reservoir. The hypothetical GCS project considered
 215 in this study treats the Vedder Sandstone, a sedimentary formation in the Southern San Joaquin
 216 Valley of CA, as a GCS system. The injection site is located approximately 20 miles northwest
 217 of Bakersfield, CA in Kern County. The region was previously characterized as part of the West-
 218 carb Kimberlina Pilot Project [23].

219
 220 Building on a previous study [13], a 50-year basin-scale injection of CO₂ and a 50-year post-
 221 injection period were simulated. CO₂ and brine leakage rates into a USDW were calculated along
 222 the 1000 wellbores in the study area, the volume of impacted aquifer for each leaky wellbore
 223 location determined, and compiled into a time-to-detection map for the entire site. We used the
 224 Monte Carlo framework of the NRAP-Open-IAM to run stochastic simulations that captured the
 225 uncertainty associated with the effective permeability of the wellbores in the model. The NRAP-
 226 Open-IAM represents discrete elements of a GCS system using individual surrogate models. Our
 227 integrated assessment model of the site consisted of a single reservoir lookup table joined with
 228 1000 individual multisegmented wellbore models connected to FutureGen2 aquifer models in a
 229 one-way forward coupling.

230
 231 In this preliminary example only a few wellbores are found to have detectable leaks, meaning
 232 only a very few locations are feasible for consideration as monitoring locations. This means that
 233 a full grid search is computationally possible, requiring only a few minutes to consider the 35,442
 234 possible combinations (Figure 5, gray dots) of 5 sensor locations. We then use a Monte Carlo

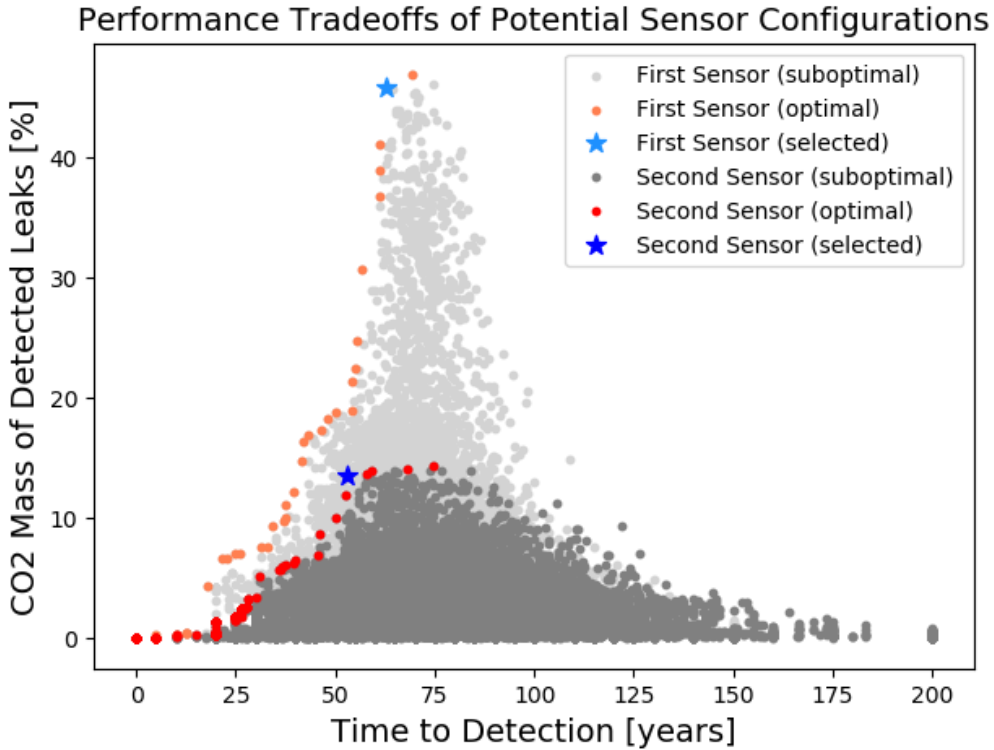


Figure 3: Each possible sensor placement is evaluated in terms of average time to detection and the percentage of leaks detected (weighted by mass of leak). Suboptimal options for the first sensor placement (light gray) are discounted because they each have worse performance than at least one other sensor location in terms of time to detection, poorer coverage or both. A single sensor placement is selected (light blue) from along the optimal tradeoff curve (orange). Suboptimal options (red) for the second sensor are then discounted in the same manner, and the second sensor placement is selected (blue) from along the new tradeoff curve (red).

235 approach to generate 10,000 random monitoring plans, and find almost the exact same monitoring
 236 performance (Figure 5a). By reducing the Monte Carlo search another order of magnitude
 237 (Figure 5b), we see that a fair number of possible monitoring outcomes are missed, however the
 238 general trend remains the same. The Simulated Annealing and Heuristic Algorithms are also
 239 compared to the grid search method (Figure 5c,d), and produce similar results.

240
 241 This demonstrates that in simple cases at least, a relatively modest Monte Carlo sampling can
 242 nearly fully explore the decision space. For more complex monitoring design problems, how-
 243 ever, a very large sample size may be required for Monte Carlo to adequately explore the decision
 244 space. This may become computationally impractical, and therefore the remaining algorithms
 245 will simply be evaluated by comparison to a "very large" Monte Carlo sampling rather than a
 246 full grid search.

247

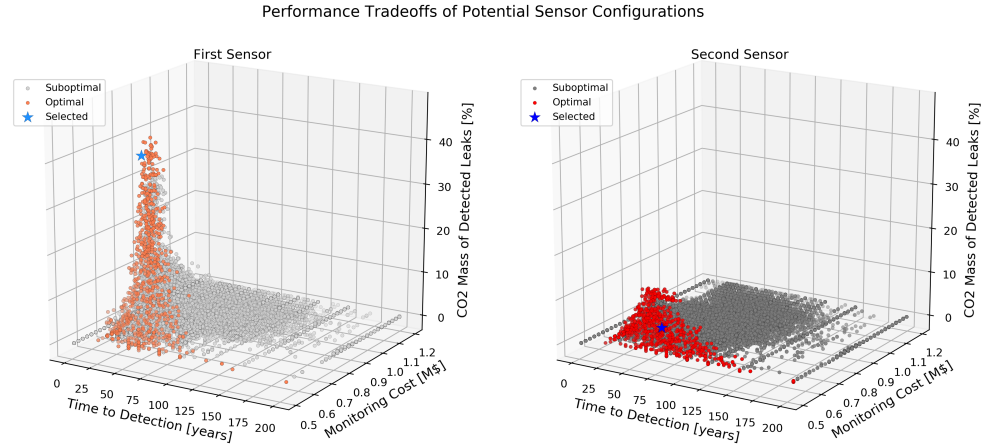


Figure 4: Each possible sensor placement is evaluated in terms of monitoring cost, average time to detection and the percentage of leaks detected (weighted by mass of leak). Suboptimal options for the first sensor placement (light gray) are discounted because they each have worse performance than at least one other sensor location in terms of time to detection, poorer coverage or both. A single sensor placement is selected (light blue) from along the optimal tradeoff curve (orange). Suboptimal options (red) for the second sensor are then discounted in the same manner, and the second sensor placement is selected (blue) from along the new tradeoff curve (red).

248 **4.2. NRAP-Open-IAM Generic Aquifer ROM**

249 The Reservoir component model provides spatial and temporal information on pressure and
 250 saturation in the storage reservoir. A reservoir simulation look-up table in United States (US)
 251 Department of Energy (DOE)'s National Risk Assessment Partnership Open-source Integrated
 252 Assessment Model (NRAP-Open-IAM) [22] is used for this study. The table is based on a set
 253 of numerical simulation models with varying rock properties for the Kimberlina reservoir in
 254 southern San Joaquin basin in California, USA. [28] The homogeneous reservoir model No.
 255 14 (reservoir porosity: 0.276; reservoir permeability: $1.585 \times 10^{-13} \text{ m}^2$; caprock permeability:
 256 $1.995 \times 10^{-18} \text{ m}^2$) for the first 100 years (i.e., 50 years of CO₂ injection at a rate of 5 million
 257 metric tons/year and 50 years of post-injection) was used.

258 Coupled to the reservoir model, a wellbore model predicts leakage amount of the injected
 259 CO₂ and formation brine to an overlying aquifer through leaky wells based on input pressure and
 260 CO₂ saturation. A caprock segment wellbore model in NRAP-Open-IAM [22] was adopted [3].
 261 This model assumes no leakage into caprock layers, and thus it provides a conservative estimate
 262 for risk evaluation. 74 wells within 5 km from the injection well were analyzed.

263 The output leakage rates of CO₂ and brine from the wellbore model is fed into a genetic
 264 aquifer impact reduced-order-model [1] as input to forecast the impacts of the well leakage on
 265 aquifers. The model generates 3D temporal and spatial datasets of mass fractions of the dissolved
 266 CO₂ and salts throughout the aquifer. The model performs individual calculation for each of
 267 wells, and once dissolved CO₂ or salts plumes from different wells are overlapped, maximum
 268 value in the cell were used.

269 For a stochastic analysis, 200 realizations of input parameters of the wellbore and aquifer
 270 models were sampled using Latin-hypercube sampling (LHS) [9]. Table 1 shows the parameter
 271 ranges used. Of these stochastically generated models, 50 represent very small leaks which never

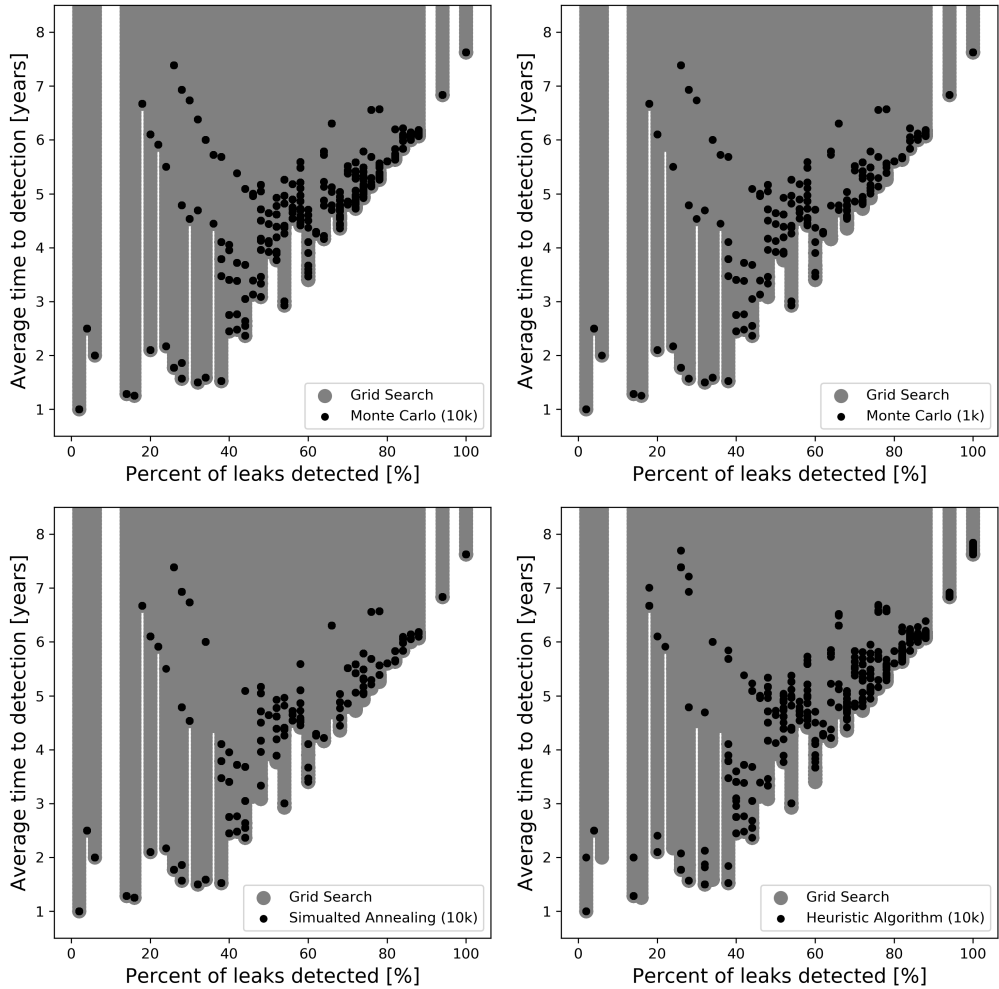


Figure 5: Comparison between Monte Carlo searches (for $n=10,000$ and $n=1,000$) and an exhaustive grid search of the decision space using the NRAP-Open-IAM Open Wellbore ROM.

272 exceed 0.01% CO₂ concentration [Figure 6] and are therefore neglected from the analysis.

273 This input dataset was run using DREAM's Monte Carlo, Simulated Annealing and Heuristic
 274 algorithms described above [Section 3.2], however due to the large size of the input files the grid
 275 search and genetic algorithm were too computationally intensive to be practical. Each of the
 276 150 input files were 800-900MB, however DREAM had a peak memory usage of 2.1GB of the
 277 machine's 16GB RAM. As working with this dataset was time-intensive, only 100 iterations
 278 were run for each algorithm. For this example [Figure 7], the Monte Carlo algorithm was able
 279 to identify one monitoring plan capable of detecting 134/150 leak scenarios using 8 monitoring
 280 wells, while the heuristic algorithm was able to detect 138/150 leak scenarios using 2 monitoring
 281 wells.

Table 1: Parameter ranges for OpenIAM Generic Aquifer model

Parameter	Unit	Minimum	Maximum
Reservoir salinity	%	0.03	0.05
Well permeability	m^2	1.0×10^{-14}	1.778×10^{-12}
Aquifer thickness	m	25	100
Aquifer top depth	m	2,000	2,500
Aquifer porosity	%	0.02	0.10
Aquifer horizontal permeability	m^2	1.0×10^{-13}	1.0×10^{-10}
Aquifer permeability anisotropy	-	0.01	1.0

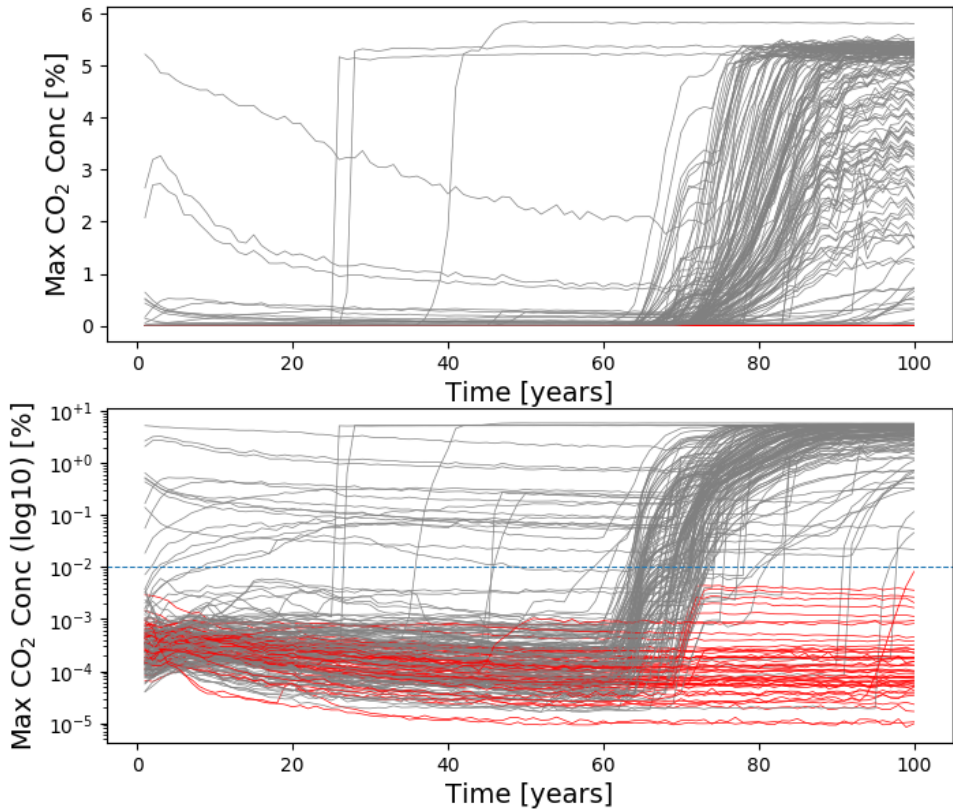


Figure 6: The maximum CO₂ concentration (taken over the entire model space) is shown for each leak in both linear-linear and linear-log space. Leaks which never exceed 0.01% CO₂ are highlighted in red and neglected from the analysis.

282 4.3. Kimberlina 1.2

283 We then ran monitoring plan optimizations based on the Kimberlina 1.2 dataset [15], sup-
 284 plemented by a gravity model later applied by Xianjin Yang. These optimizations considered
 285 combinations of pressure and saturation sensors installed within wellbores, as well as gravity

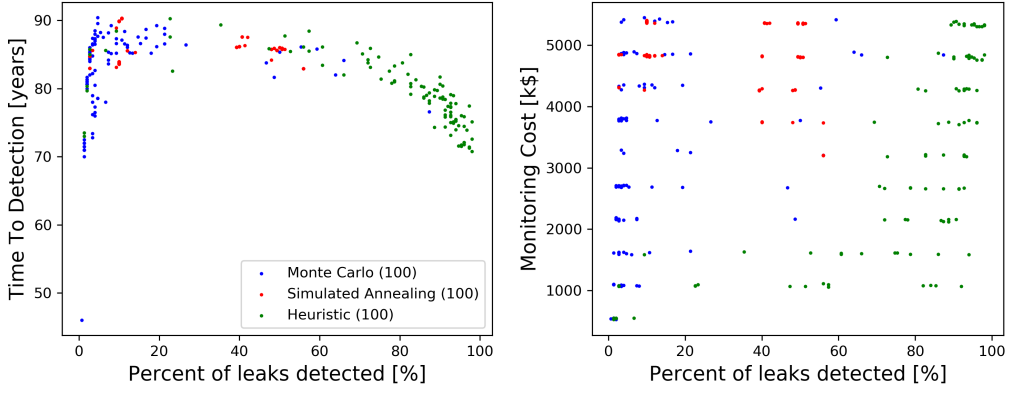


Figure 7: Comparison between the performance of Monte Carlo, Simulated Annealing and Heuristic algorithm using the OpenIAM Aquifer simulation dataset.

286 surveys. The spatial extent and resolution of this case allows us to consider many more (+3500)
 287 possible sensor locations, and combinations of as many as 5 sensors were considered. As the
 288 grid search method would therefore require an astronomical amount of computational effort, a
 289 large (100,000) set of Monte Carlo iterations were compared to 1,000 iterations of our heuristic
 290 algorithm. The heuristic algorithm produced much better results than either the Monte Carlo or
 291 Simulated Annealing algorithms, with some plans detecting more than 99.7% of the total CO₂
 292 leakage potential, while maintaining a relatively low cost and time to detection.
 293

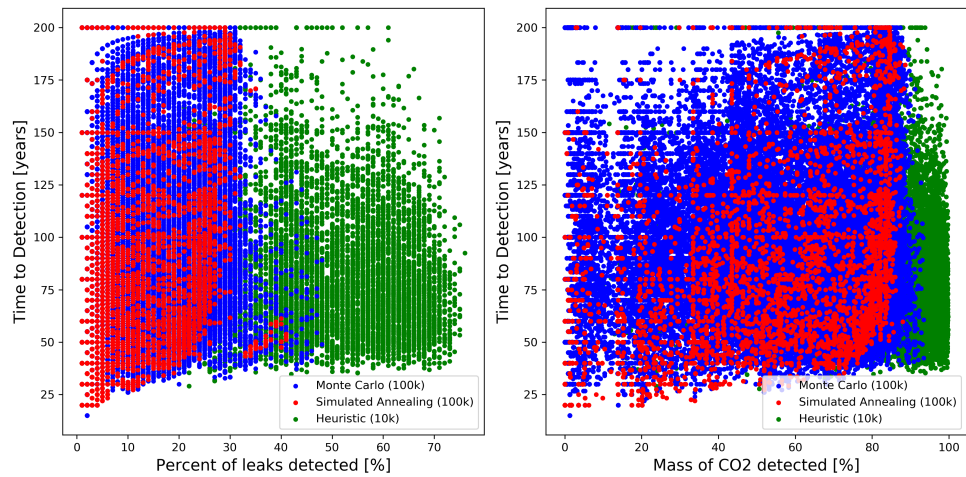


Figure 8: Comparison between the performance of Monte Carlo, Simulated Annealing and the DREAMv3 heuristic algorithm using the Kimberlina 1.2 leakage simulation dataset.

294 The best-performing monitoring plans were then identified [blue dots, Figure 10b], having
 295 greater than 98% detection of CO₂ leakage by mass, and minimal monitoring costs and time to

296 detection. This pool of candidates can then be viewed one at a time and examined with an eye
 297 for practical field deployment. If the optimal monitoring plans are deemed viable for real-world
 298 application, they can be implemented, otherwise the algorithm can be run for additional iterations
 299 or using a different algorithm.

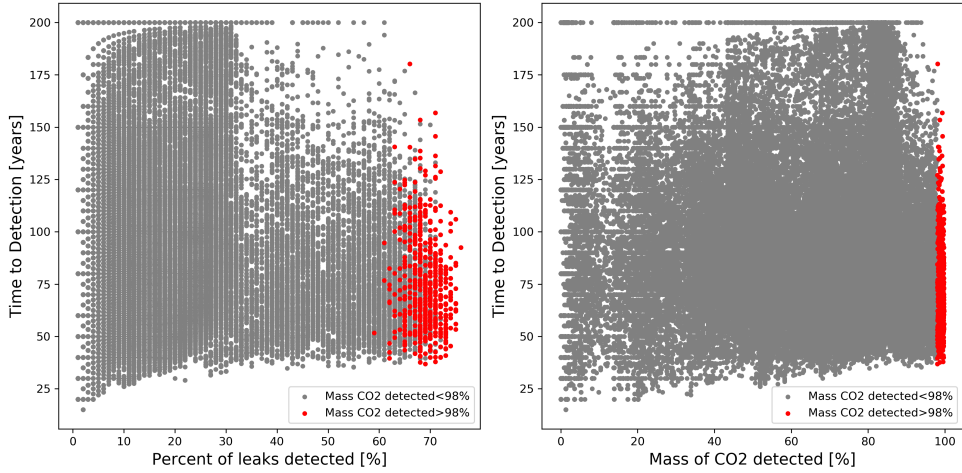


Figure 9: Monitoring plans with >98% mass CO2 detection are highlighted in red

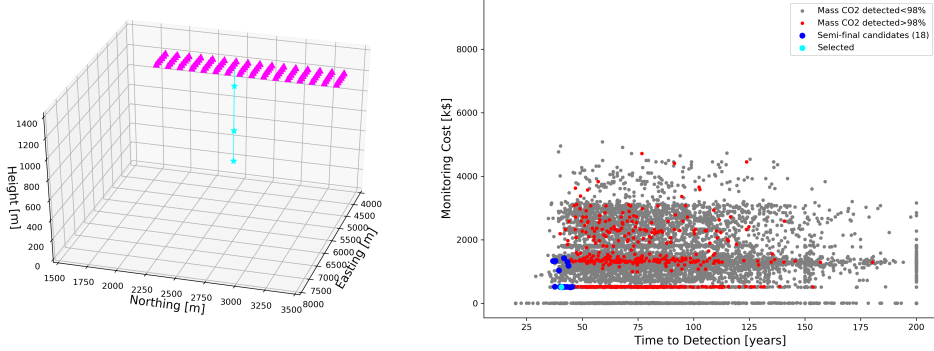


Figure 10: Set of optimal monitoring plan candidates

300 5. Conclusion

301 The DREAM software tool takes as input a set of (unlikely) CO₂ leakage scenarios and de-
 302 signs a monitoring plan tailored to the risk profile of the site. The current generation (version
 303 3.0) of the software includes a heuristic algorithm which produces much cheaper and more ef-
 304 fective monitoring plans while still providing a range of possible tradeoffs for the user to decide
 305 from. This version also includes passive surface geophysics data types such as gravity surveys,
 306 optimizing the survey size and station density.

307 **References**

308 [1] Diana H Bacon. Nrap-open-iam: Generic aquifer component development and testing. Technical report, Pacific
309 Northwest National Lab.(PNNL), Richland, WA (United States), 2022.

310 [2] Diana H Bacon, Catherine MR Yonkofski, Christopher F Brown, Deniz I Demirkarli, and Jonathan M Whiting.
311 Risk-based post injection site care and monitoring for commercial-scale carbon storage: Reevaluation of the fu-
312 turegen 2.0 site using nrap-open-iam and dream. *International Journal of Greenhouse Gas Control*, 90:102784,
313 2019.

314 [3] S. Baek, D.H. Bacon, and N.J. Huerta. Deep learning-based multisegmented wellbore model development for many
315 wells site study. In *NRAP Annual Technical Meeting Conference*. National Risk Assessment Partnership, 2022.

316 [4] Kalyanmoy Deb. A fast and elitist multiobjective genetic algorithm: Nsga-ii. *IEEE Transactions on Evolutionary
317 Computation*, 6(2):182–197, 2002.

318 [5] Anirban Dhar and Bithin Datta. Multiobjective design of dynamic monitoring networks for detection of ground-
319 water pollution. *Journal of water resources planning and management*, 133(4):329–338, 2007.

320 [6] Anirban Dhar and Bithin Datta. Logic-based design of groundwater monitoring network for redundancy reduction.
321 *Journal of water resources planning and management*, 136(1):88–94, 2010.

322 [7] Anirban Dhar and Rajvardhan S Patil. Multiobjective design of groundwater monitoring network under epistemic
323 uncertainty. *Water resources management*, 26(7):1809–1825, 2012.

324 [8] Paul F Hudak and Hugo A Loaiciga. An optimization method for monitoring network design in multilayered
325 groundwater flow systems. *water resources research*, 29(8):2835–2845, 1993.

326 [9] Ronald L Iman, Jon C Helton, and James E Campbell. An approach to sensitivity analysis of computer models:
327 Part i—introduction, input variable selection and preliminary variable assessment. *Journal of quality technology*,
328 13(3):174–183, 1981.

329 [10] Abdelhaleem I Khader and Mac McKee. Use of a relevance vector machine for groundwater quality monitoring
330 network design under uncertainty. *Environmental modelling & software*, 57:115–126, 2014.

331 [11] Scott Kirkpatrick, C Daniel Gelatt Jr, and Mario P Vecchi. Optimization by simulated annealing. *science*, 220
332 (4598):671–680, 1983.

333 [12] Joshua B Kollat, Patrick M Reed, and Joseph R Kasprzyk. A new epsilon-dominance hierarchical bayesian opti-
334 mization algorithm for large multiobjective monitoring network design problems. *Advances in Water Resources*,
335 31(5):828–845, 2008.

336 [13] Greg Lackey, Veronika S. Vasylkivska, Nicolas J. Huerta, Seth King, and Robert M. Dilmore. Managing well
337 leakage risks at a geologic carbon storage site with many wells. *International Journal of Greenhouse Gas Control*,
338 88:182–194, 2019. ISSN 17505836. doi: 10.1016/j.ijggc.2019.06.011.

339 [14] Qiankun Luo, Jianfeng Wu, Yun Yang, Jiazhong Qian, and Jichun Wu. Multi-objective optimization of long-term
340 groundwater monitoring network design using a probabilistic pareto genetic algorithm under uncertainty. *Journal
341 of Hydrology*, 534:352–363, 2016.

342 [15] Kayyum Mansoor, Thomas A Buscheck, Xianjin Yang, Susan A Carroll, and Xiao Chen. Llnl kimberlina 1.2 nuft
343 simulations june 2018 (v2). Technical report, National Energy Technology Laboratory (NETL), Pittsburgh, PA,
344 Morgantown, WV . . . , 2020.

345 [16] Nicholas Metropolis, Arianna W Rosenbluth, Marshall N Rosenbluth, Augusta H Teller, and Edward Teller. Equa-
346 tion of state calculations by fast computing machines. *The journal of chemical physics*, 21(6):1087–1092, 1953.

347 [17] LM Nunes, MC Cunha, and L Ribeiro. Groundwater monitoring network optimization with redundancy reduction.
348 *Journal of Water Resources Planning and Management*, 130(1):33–43, 2004.

349 [18] LM Nunes, MC Cunha, and L Ribeiro. Optimal space-time coverage and exploration costs in groundwater moni-
350 toring networks. *Environmental monitoring and assessment*, 93(1-3):103–124, 2004.

351 [19] Om Prakash and Bithin Datta. Sequential optimal monitoring network design and iterative spatial estimation
352 of pollutant concentration for identification of unknown groundwater pollution source locations. *Environmental
353 monitoring and assessment*, 185(7):5611–5626, 2013.

354 [20] Patrick Reed, Joshua B Kollat, and VK Devireddy. Using interactive archives in evolutionary multiobjective op-
355 timization: A case study for long-term groundwater monitoring design. *Environmental Modelling & Software*, 22
356 (5):683–692, 2007.

357 [21] J Sreekanth and Bithin Datta. Simulation-optimization models for the management and monitoring of coastal
358 aquifers. *Hydrogeology Journal*, 23(6):1155–1166, 2015.

359 [22] Veronika Vasylkivska, Robert Dilmore, Greg Lackey, Yingqi Zhang, Seth King, Diana Bacon, Bailian Chen,
360 Kayyum Mansoor, and Dylan Harp. Nrap-open-iam: A flexible open-source integrated-assessment-model for
361 geologic carbon storage risk assessment and management. *Environmental Modelling & Software*, 143:105114,
362 2021.

363 [23] Haruko M. Wainwright, Stefan Finsterle, Quanlin Zhou, and Jens T. Birkholzer. Modeling the performance of

364 large-scale co₂ storage systems: A comparison of different sensitivity analysis methods. *International Journal of*
365 *Greenhouse Gas Control*, 17:189–205, 2013. ISSN 17505836. doi: 10.1016/j.ijggc.2013.05.007.

366 [24] Jianfeng Wu, Chunmiao Zheng, Calvin C Chien, and Li Zheng. A comparative study of monte carlo simple genetic
367 algorithm and noisy genetic algorithm for cost-effective sampling network design under uncertainty. *Advances in*
368 *Water Resources*, 29(6):899–911, 2006.

369 [25] Catherine Yonkofski, G Tartakovsky, N Huerta, and A Wentworth. Risk-based monitoring designs for detecting
370 co₂ leakage through abandoned wellbores: An application of nrp's wlat and dream tools. *International Journal of*
371 *Greenhouse Gas Control*, 91:102807, 2019.

372 [26] Catherine MR Yonkofski, Jason A Gastelum, Ellen A Porter, Luke R Rodriguez, Diana H Bacon, and Christopher F
373 Brown. An optimization approach to design monitoring schemes for co₂ leakage detection. *International Journal*
374 *of Greenhouse Gas Control*, 47:233–239, 2016.

375 [27] Catherine MR Yonkofski, Casie L Davidson, Luke R Rodriguez, Ellen A Porter, Sadie R Bender, and Christopher F
376 Brown. Optimized, budget-constrained monitoring well placement using dream. *Energy Procedia*, 114:3649–3655,
377 2017.

378 [28] Quanlin Zhou and Jens T Birkholzer. On scale and magnitude of pressure build-up induced by large-scale geologic
379 storage of co₂. *Greenhouse Gases: Science and Technology*, 1(1):11–20, 2011.